

DETAILED X-RAY OBSERVATIONS OF M83

G. TRINCHIERI,¹ G. FABBIANO,¹ AND G. G. C. PAULUMBO²

Received 1984 June 18; accepted 1984 September 6

ABSTRACT

M83 is detected in X-rays with the *Einstein Observatory* with an X-ray luminosity of $\sim 6 \times 10^{39}$ ergs s⁻¹ (0.5–3.0 keV, for a distance of 3.75 Mpc). The extent and shape of the X-ray emission are comparable to those in the optical (blue band), although the inner 2' region shows a relative X-ray excess. This excess could be accounted for by a clustering of bulge-type X-ray sources in the inner region of the plane of the galaxy, analogous to what is observed in M31 and in the Milky Way.

High-resolution X-ray observations show no strong correlation between the X-ray emission and the spiral arm pattern. This suggests that most of the X-ray emission from the plane of M83 is due to unresolved sources belonging to the "smooth" disk population with ages in the range 10⁸–10⁹ yr.

Six bright sources, each with $L_x > 1 \times 10^{38}$ ergs s⁻¹, are detected in the plane and near the nuclear region of M83. Although they do not have any obvious optical counterpart, their high X-ray luminosities suggest that they are close accreting binaries. The starburst nucleus of M83 is detected with $L_x \approx 2 \times 10^{39}$ ergs s⁻¹. The X-ray to optical flux ratio (f_x/f_B) of the nuclear region is significantly lower than the f_x/f_B of the main body of the galaxy and much lower than those of blue starburst galaxies detected in X-rays, suggesting a lack of massive binary X-ray sources. This indicates that the age of the burst of star formation is of the order of 10⁷ yr.

If, as in the starburst nuclei of M82 and NGC 253, hot gas is being ejected from the nuclear region of M83, the X-ray luminosity of the nucleus of M83 could be as low as $\sim 4 \times 10^{38}$ ergs s⁻¹. Given the observed X-ray to optical flux ratio, an upper limit on the extinction in the nuclear region of $A_v < 15$ mag can be set.

Subject headings: galaxies: individual — galaxies: structure — stars: formation — X-rays: sources

I. INTRODUCTION

The galaxy M83 (= NGC 5236) is a bright nearby southern spiral galaxy (R.A. [1950] = 13^h34^m17, decl. [1950] = -29°36'8), classified as a SAB(S)c I-II (de Vaucouleurs, de Vaucouleurs, and Corwin 1976). The galaxy is seen almost face on ($i = 24^\circ$; Talbot, Jensen and Dufour 1979) and has a corrected isophotal diameter $D_0 = 16.2$ (Talbot, Jensen, and Dufour 1979). The most recent estimate of its distance is 3.75 Mpc (de Vaucouleurs 1979). Evidence for a barlike structure is seen in the nuclear and inner arms region. The nuclear region is optically bright and amorphous (Sersic and Pastoriza 1967) and is also a bright and extended source at radio (Condon *et al.* 1982), infrared (Telesco and Harper 1980) and ultraviolet (Bohlin *et al.* 1983; W. Wamsteker and G. G. C. Paulumbo, in preparation) frequencies. From the analysis of these observations, these authors suggested that the nuclear region is the site of active star formation. Detailed optical photometric and spectroscopic observations of M83 have been made to study the distribution and age of the stellar population and the rate of star formation in the plane and arms of the galaxy (Talbot, Jensen, and Dufour 1979; Dufour *et al.* 1980; Jensen, Talbot, and Dufour 1981; de Vaucouleurs, Pence, and Davoust 1983). A very large number of newly formed massive stars was found in the inner 150" region. The young stars rather uniformly fill the inner spiral arms (Jensen, Talbot, and Dufour 1981).

Therefore, M83 is a very interesting target for X-ray observations. Since M83 is seen face on, the emission from the starburst nucleus can be resolved from the plane emission and studied separately. X-ray observations of the edge-on galaxy

NGC 253 (Fabbiano and Trinchieri 1984) and M82 (Watson, Stanger, and Griffiths 1984) have provided evidence that the region of the starburst nucleus is a strong X-ray source with complex morphology. Moreover, high-resolution X-ray observations provide a unique opportunity to study the distribution of X-ray sources in the plane and arms of a spiral galaxy similar to the Milky Way (Jensen, Talbot, and Dufour 1981) and to correlate them with the stellar population.

M83 was first observed in X-rays with the *Einstein Observatory* Imaging Proportional Counter (IPC; for a description of the *Einstein* instrument, see Giacconi *et al.* 1979) as part of a sample of late-type spiral galaxies (Fabbiano, Trinchieri, and Macdonald 1984).³ Two high-resolution X-ray observations were subsequently obtained with the High Resolution Imager (HRI). In this paper, the IPC image is used to study the overall distribution of the X-ray surface brightness. The higher spatial resolution HRI data are used to study the nuclear region and the detailed distribution of the X-ray emission in the inner regions of the plane and in the spiral arms of M83.

II. DATA ANALYSIS

M83 was observed with the IPC in 1979 July/August for ~ 6000 s. It was observed twice with the HRI in 1980 January and 1981 February for a total time of $\sim 44,600$ s. The parameters of the observations are summarized in Table 1.

a) IPC Observation

The image was processed with the revised IPC processing system (REV 1; Harnden *et al.* 1984). The new image thus

³ Fabbiano, Trinchieri, and Macdonald (1984) quote a luminosity of 1.6×10^{40} ergs s⁻¹. This is a different value from that obtained here because of (a) a different choice of the distance (6.7 Mpc) and (b) a smaller radius $R_0(5'6)$ used to integrate the counts from the galaxy.

¹ Harvard-Smithsonian Center for Astrophysics.

² Istituto T.E.S.R.E./CNR.

TABLE 1
EINSTEIN X-RAY OBSERVATIONS OF M83

Instrument	Sequence Number	Observation Time (s)	Date of Observation	Field Center (α , δ)
IPC	588	5922	1979 Jul 31–Aug 1	13 ^h 34 ^m 10 ^s .17 –29°36' 43".4
HRI	587	24575	1980 Jan 15–16	13 34 10.14 –29 36 46.4
	10447	20003	1981 Feb 13	13 34 10.14 –29 36 46.4

obtained is 1400 s shorter than that used by Fabbiano, Trinchieri, and Macdonald (1984), but it is cleaned of contaminating emission from the South Atlantic Anomaly and the “bright Earth” and has been corrected using improved instrument calibration and aspect solution software.

i) M83

Contour maps of the central region of the IPC field were produced from the data smoothed with a Gaussian function with $\sigma = 30''$. Iso-intensity contours of the X-ray emission are shown in Figure 1 for different energy channels (0.2–0.8, 0.8–3.5, and 0.2–3.5 keV). The background has been modeled from a template obtained from IPC observations of deep survey fields and bright Earth emission combined to best reproduce the background for this image (Harden *et al.* 1984).

The X-ray emission appears extended and peaked on the nucleus of the galaxy. No significant differences are found in maps at different energies, except for a very soft source (I3 in Table 2) NW of the nucleus (Fig. 1a). The standard detection algorithm finds one source on a spiral arm SE of the nucleus (I2 in Table 2). Two more peaks of emission (Source I4 and I5 in Table 2) are also seen at the outskirts of the galaxy (see Fig. 1). Since they are weak and within the extended emission of M83 the “local detect” algorithm cannot detect them.

The X-ray positions and net counts for the whole galaxy and for the individual sources are listed in Table 2 (sources I1–I5). For source I1 (the whole galaxy) all the counts inside the optical radius R_0 of M83 ($R_0 = 8'$) are given. For the other sources in M83 a radius of $2'$ was used. This radius was chosen as a compromise between the need of a small cell size, in order not to include too much of the extended galaxy emission, and the spread due to the IPC Point Response Function. About 85% of the counts of a point source are contained within $2'$ radius. The fluxes and luminosities for sources I2–I5 have been corrected for this. The fluxes listed in Table 2 are calculated using a thermal bremsstrahlung spectrum with $kT = 5$ keV and an absorbing column $N_H = 5 \times 10^{20} \text{ cm}^{-2}$ for absorption in our galaxy (Heiles 1975). The background has been estimated from the template discussed above. If the diffuse galaxy emission is subtracted from sources I2–I5, the resulting net counts would be ~ 61 for source I2, but < 10 for the other sources. However, source I3 is detected only in the very soft channels, which indicates that it has a different spectrum than the diffuse emission and is therefore likely to be a real source. Sources I4 and I5 may instead just be local peaks in the diffuse galactic emission.

Power-law and thermal bremsstrahlung spectra were fitted to the central source, using the data within the inner $3'$ region, for which accurate gain determination and good statistics are available. About 400 net counts are contained in such regions. However, the IPC gain varied from BAL ~ 19 to BAL ~ 12

during the observation. Therefore no significant constraints can be determined on either the power-law index or the temperature nor on the absorbing column N_H . Only hardness ratios (H.R.) are given in Table 2. The hardness ratio is defined

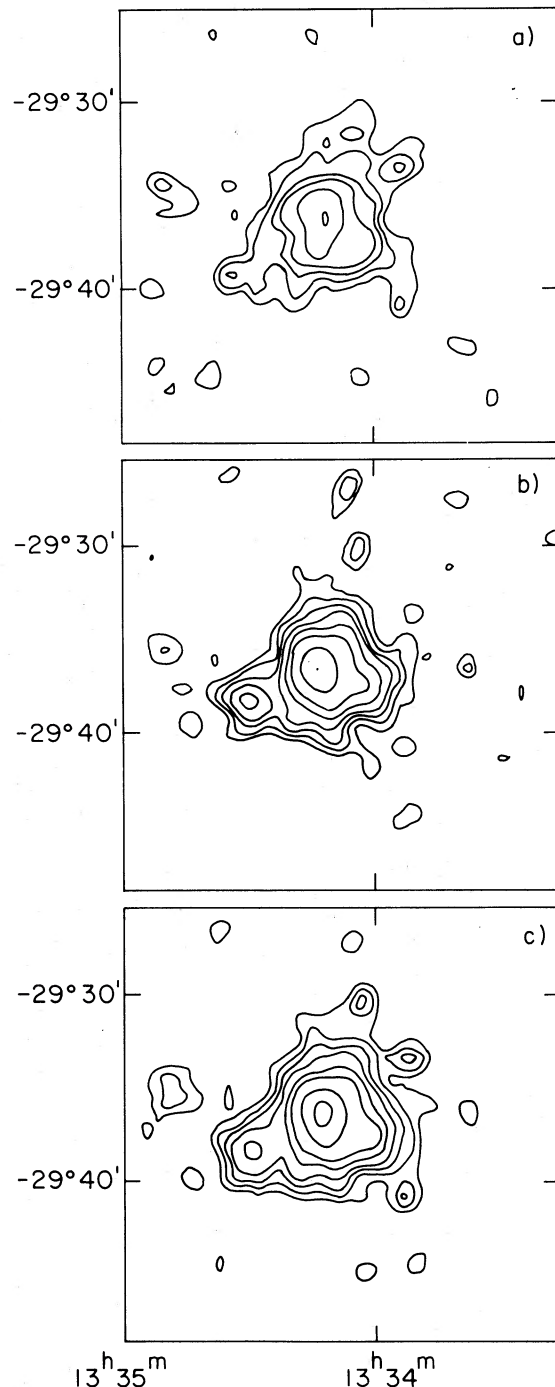


FIG. 1.—X-ray contours of the IPC observations of M83. Different energy channels have been used: (a) 0.2–0.8 keV; (b) 0.8–3.5 keV; (c) 0.2–3.5 keV. The data have been smoothed with a $30''$ Gaussian. The first contour plotted is a 2σ level over the background. The values for the contours are: (a) $(4.0, 6.5, 9.6, 13.0, 21.5, 31.3) \times 10^{-4}$ counts arcsec^{-2} ; (b) $(4.0, 6.5, 9.6, 13.1, 20.9, 30.8, 55.7, 86.7) \times 10^{-4}$ counts arcsec^{-2} ; (c) $(5.6, 9.0, 12.7, 17.1, 27.0, 38.7, 67.1, 102.1) \times 10^{-4}$ counts arcsec^{-2} . The FWHM of the beam is 2.3 for the 0.2–3.5 keV energy range (Fig. 1c). This beam is the result of the convolution of the IPC point response function with a $30''$ Gaussian.

TABLE 2
X-RAY SOURCES DETECTED BY THE IPC IN THE M83 FIELD

Source Number	R.A., Decl.	Radius (arcmin)	Net Counts/ Error	H.R./ Error	$f_x(0.5-3.0 \text{ keV})^a$ $L_x(0.5-3.0 \text{ keV})$	Notes
I1.....	13 ^h 34 ^m 14 ^s -29°36' 24"	8	774.4 ±36.7	1.9 ±0.2	3.4×10^{-12} 5.7×10^{39}	Whole galaxy
I2.....	13 34 30 -29 38 21	2	80. ±10.8	1.5 ±0.4	4.2×10^{-13} 6.9×10^{38}	Corresponding to HRI source H2
I3.....	13 33 54 -29 33 25	2	24.9 ±7.9	0.3 ±0.3	1.3×10^{-13} 2.2×10^{38}	Soft source
I4.....	13 34 04 -29 30 25	2	24.4 ±7.6	1.0 ±0.7	1.3×10^{-13} 2.2×10^{38}	May be only a local peak in diffuse emission; see text.
I5.....	13 33 55 -29 40 50	2	24.9 ±7.5	1.3 ±0.8	1.3×10^{-13} 2.3×10^{38}	May be only a local peak in diffuse emission; see text.
I6.....	13 32 41 -29 35 24	3	440.2 ±23.4	2.5 ±0.3	3.2×10^{-12}	Compact object?
I7.....	13 35 16 -29 28 39	3	62.1 ±13.4	2.0 ±0.8	4.0×10^{-13} 7.0×10^{43}	Background cluster
I8.....	13 35 54 -29 18 31	3	83.0 ±12.1	1.0 ±0.4	6.6×10^{-13}	SAO star; $m = 5.84$
I9.....	13 32 8 -29 40 00	2	40.1 ±7.5	1.7 ±0.7	3.0×10^{-13}	Star; $m = 9.0$

^a Assuming $kT = 5 \text{ keV}$ and $N_H = 5 \times 10^{20} \text{ cm}^{-2}$.

as the ratio of net counts in the 0.8–3.5 keV band to those in the 0.2–0.8 keV band. Each source (except I3) has a H.R. between 1 and 2, although with large errors, showing that it is not particularly soft or highly absorbed.

ii) Other Sources in the Field

Four more sources were found in the IPC field. Their positions and fluxes are listed in Table 2. To calculate the flux the net counts within a circle of 3' radius were used for sources I6–I8. Because Source I9 is very close to the IPC support structure (the “ribs”), a smaller radius of 2' was used. These sources are located ~ 2 optical radii or more away from the nucleus of M83. In Figure 2 the finding charts for these sources are presented. A pointlike object can be seen in the error circle of the X-ray source I6. A deep CCD picture of this field, taken by R. Schild, shows a background cluster at the position of source I7. The brightest galaxy in the cluster has a redshift of $z = 0.189$ measured by J. Danziger (I. Gioia 1984, private communication). This implies an X-ray luminosity $L_x = 7 \times 10^{43} \text{ ergs s}^{-1}$ (for $H_0 = 50 \text{ km s}^{-1} \text{ Mpc}^{-1}$), consistent with the X-ray luminosity of clusters of galaxies (see Jones and Forman 1984). Bright stars are found in the error circles of both sources I8 and I9. The star SAO 181825 (R.A. [1950.0] = 13^h35^m53^s.056, decl. [1950.0] = -29°18'22".9) lies $\sim 15''$ away from the centroid of the X-ray source I8 (see Table 2 and Fig. 2) well within the IPC error circle ($\sim 30''$). Its visual magnitude is $m_v = 5.84$, and its spectral type is F0. If the star is the optical counterpart of source I8, the ratio of X-ray band flux to V band flux (f_x/f_v , as defined in Topka *et al.* 1982) is 4.25×10^{-5} , in the range observed for main-sequence F stars (Topka *et al.* 1982). Therefore this star is most likely the optical identification for the X-ray source I8. The 9th mag star (Fig. 2) is likely to be the optical counterpart of source I9. Although no optical spectral information is available, the f_x/f_v is $\sim 3.5 \times 10^{-4}$, in the range of observed f_x/f_v for stars (Vaiana *et al.* 1981).

b) HRI Observations

Two observations with the High Resolution Imager (HRI) were obtained about 1 yr apart (see Table 1). Two sources

are detected in each observation by the standard processing software, one at the position of the nucleus of M83 and the other 4/6 SE of the nucleus. This second source is coincident with the IPC source I2. The two HRI images do not show significant differences except for a relative offset of $\sim 7''$ for the position of the sources. This offset could be due to uncertainty in the different boresight corrections applied to the two observations. The second observation was obtained at the end of the mission after a long failure of the satellite; a set of less accurate boresight parameters must be applied to observations obtained after this failure. After correcting for this offset, we merged the two images and used the resulting image for further analysis.

Figure 3 (Plate 1) shows the X-ray contour map obtained by smoothing the merged HRI field with a Gaussian of $\sigma = 24''$. The X-ray data are overlaid on a high-contrast blue picture of M83 (courtesy of Dr. G. de Vaucouleurs). The wide smoothing function enhances the low surface brightness emission from the plane of the galaxy. The total number of counts inside the contour defining 1σ above the average field background corresponds to an X-ray luminosity of $8 \times 10^{39} \text{ ergs s}^{-1}$ (0.5–3.0 keV), which is comparable to the total emission found inside the optical radius with the IPC (see Table 2). A discrete source coincident with the IPC source I2 can be seen on a spiral arm to the SE.

A higher resolution X-ray map of the nuclear region of M83 is shown in Figure 4. The data were smoothed with a Gaussian of $\sigma = 3''$. The background was calculated locally and subtracted from the image. In addition to the nuclear source, two unresolved sources can be seen in the figure.

The sources detected in the merged HRI field are listed in Table 3. Because of the uncertainty in the boresight correction discussed above, the error in each X-ray position of Table 3 is estimated to be $\sim 7''$. The net counts listed in Table 3 for the three unresolved sources are the background subtracted counts within an $18''$ radius circle. For the nuclear source the net counts inside the 1σ contour of Figure 4 (not plotted) are given. The background has been calculated within the central $2 \times 2 \text{ arcmin}^2$ of the image. The fluxes were calculated assuming the same spectral parameters used for the IPC

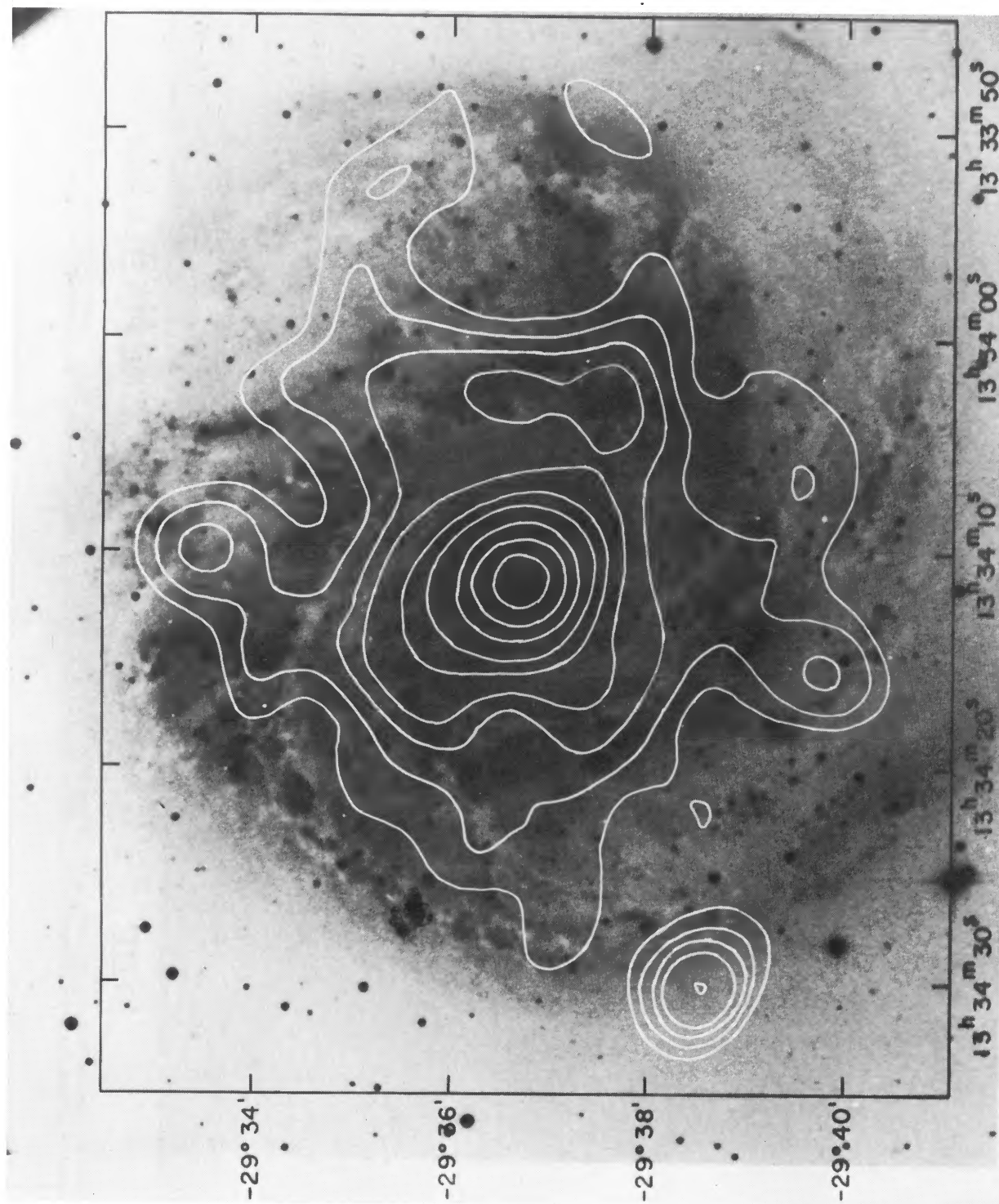
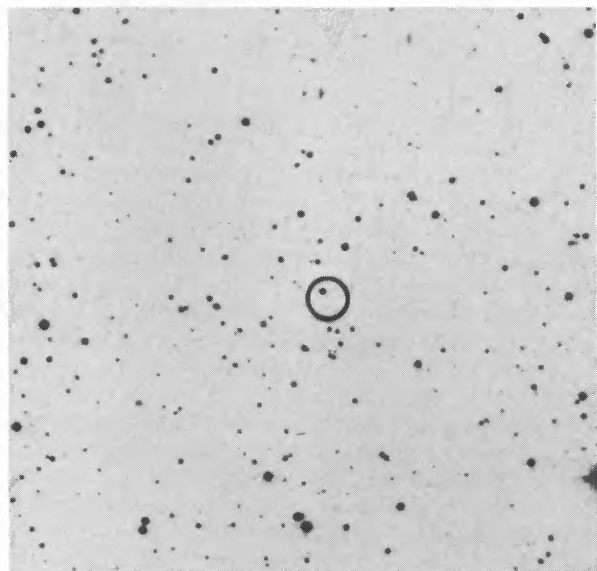


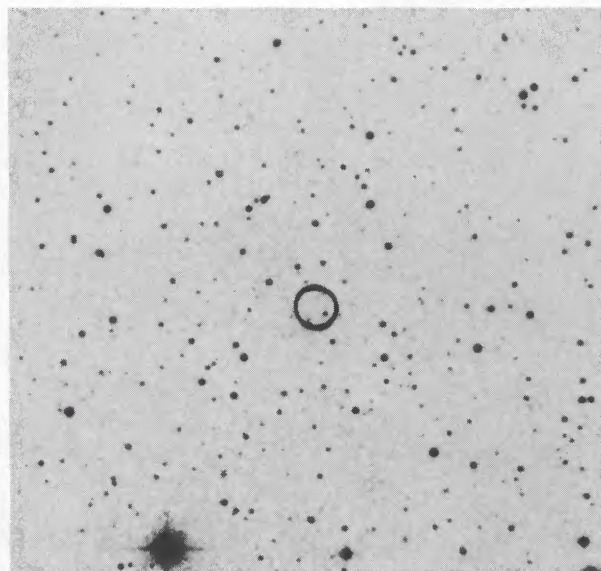
FIG. 3.—HRI X-ray contours are overlaid onto an optical picture of M83 (courtesy of Dr. G. de Vaucouleurs; see de Vaucouleurs, Pence, and Davoust 1983, Fig. 1). The X-ray data have been smoothed with a Gaussian function with $\sigma = 24''$. The first contour plotted is a 2σ level over the background and corresponds to 1.5×10^{-2} counts arcsec^{-2} . Contours of 3, 4, 5, 6, 7, 9, 11, 13 σ are then plotted.

TRINCHIERI, FABBIANO, AND PALUMBO (see page 98)

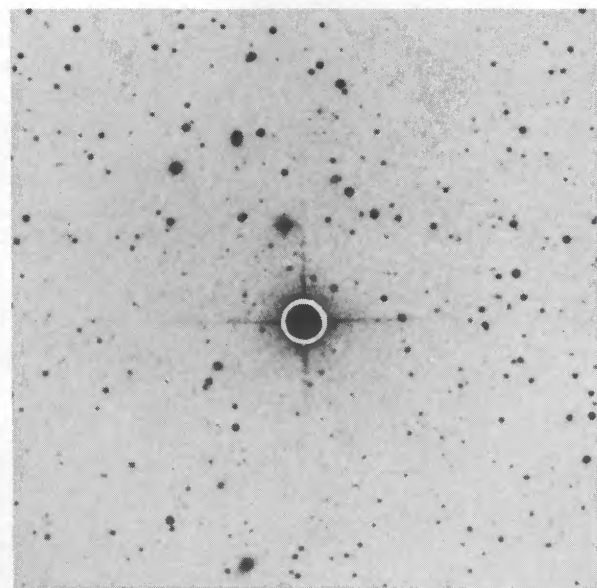
NORTH



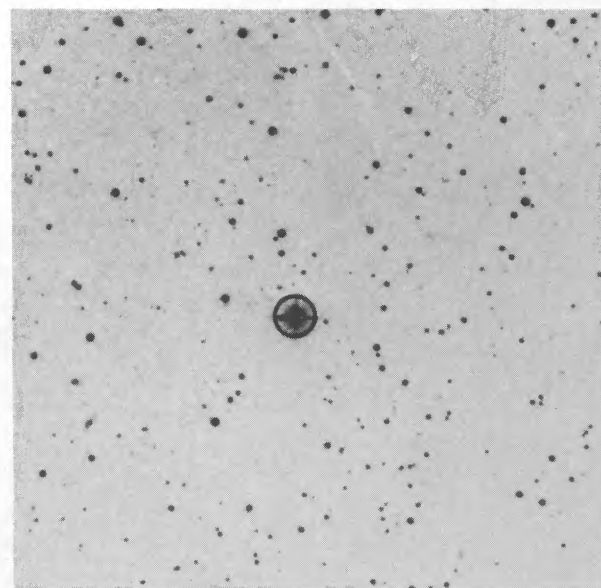
I6



I7



I8



I9

FIG. 2.—Finding charts for the serendipitous sources detected in the IPC field. The circles have 1' diameter, corresponding to the 90% confidence error in the IPC positions.

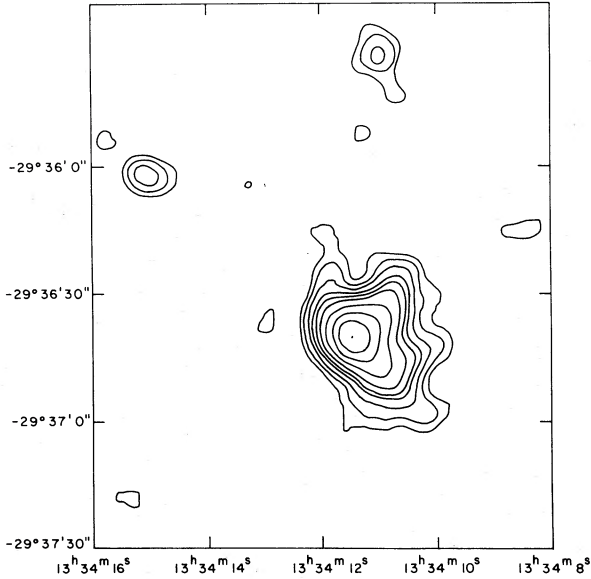


FIG. 4.—The X-ray contours of the nuclear region of M83. A $3''$ σ Gaussian function has been used to smooth the data. The first contour plotted is a 2σ level over the background and corresponds to 5.6×10^{-3} counts arcsec $^{-2}$. Contours of 3, 4, 5, 6, 7, 9, 11, 13, 15 σ are then plotted.

sources. The HRI flux of source H2 (coincident with the IPC source I2) is consistent with the flux obtained with the IPC.

The IPC sources I3, I4, and I5 are not detected in the HRI field. If their IPC counts are scaled by the ratio of IPC to HRI count for source I2, 17 counts for each source are expected in the HRI observations. This is consistent with the 3σ upper limit of 21 counts that is derived at the position of those sources.

The X-ray source coincident with the nuclear region of M83 appears extended (Fig. 4). Its extent is confirmed by the comparison of the X-ray surface brightness radial profile of this region with the HRI Point Response Function. The radial profile was obtained by binning the data in eight concentric annuli centered at the X-ray centroid. The width of each of the four inner annuli is $2''$; that of the outer four annuli is $4''$. A χ^2 test gives a probability $P < 1 \times 10^{-4}$ that the HRI Point Response Function fits the radial profile of the nuclear region. The convolution of a Gaussian function with $\sigma = 4''.5 \pm 1''.0$ with the HRI Point Response Function provides a good fit to the radial profile of this region. However, a discontinuity

between the HRI preamplifiers (“gap”) crosses the source in both images. Imperfections in the software procedure used to remove the gaps *might* introduce distortions in the final image that could be interpreted as extent. Since it is not yet known what the size and shape of these distortions might be, we prefer not to make any definite *quantitative* statement about the extent of the nuclear region.

c) X-Ray Surface Brightness Profile

To further investigate the spatial extent of the X-ray surface brightness (Σ_x) of M83, a radial profile was produced by combining the IPC and HRI observations. The composite profile is shown in Figure 5a. It consists of the higher resolution HRI surface brightness profile for the inner region of the galaxy (from the nuclear region out to $\sim 180''$) and of the lower resolution IPC surface brightness profile from $160''$ to $480''$. To produce this radial profile and to find the appropriate normalization between the two instruments, the following procedure was followed. First, the IPC radial profile was produced by binning the background-subtracted IPC data in concentric annuli about the X-ray centroid (R.A. = $13^{\text{h}}34^{\text{m}}14^{\text{s}}$, decl. = $-29^{\circ}36'24''$). The width of each annulus was $20''$ in the region from the X-ray centroid out to $140''$, then $40''$ in the region from $140''$ to $320''$, and $80''$ for the last two bins. This was necessary to ensure reasonable count statistics in each bin, given the decline of the X-ray surface brightness in the outer regions. Then, in order to model the HRI source as it would be seen with the IPC, an HRI radial profile was produced by binning the background subtracted HRI data in concentric annuli with $20''$ widths and was convolved with the IPC Point Response Function. The IPC Point Response Function was approximated by a Gaussian of $\sigma = 51''$. The profile thus obtained was compared to the actual data of the IPC radial profile using a minimum χ^2 test. In order to take into account the errors in both profiles, an error estimated from the combination of the errors in the IPC and HRI data was associated to the IPC data points. Varying the normalization constant, a minimum $\chi^2 = 13$ for 10 degrees of freedom was obtained, which indicates that the HRI and IPC profiles are statistically consistent in the inner $\sim 220''$ region. The composite profile shown in Figure 5a was then produced using the normalization constant corresponding to the minimum χ^2 and substituting the unconvolved HRI profile in the inner $160''$.

A similar composite optical (B band) surface brightness profile (Σ_B) was produced from the blue photometric data of Talbot, Jensen, and Dufour (1979). This profile, shown in

TABLE 3
X-RAY SOURCES DETECTED BY THE HRI IN M83

Source Number	R.A., Decl.	Radius (arcsec)	Net Counts/ Error	$f_x(0.5-3.0 \text{ keV})^a$ $L_x(0.5-3.0 \text{ keV})$	Notes
H1	13 ^h 34 ^m 11 ^s .41 -29°36' 39".5	22.8	268.1 ±20.2	1.2×10^{-12} 2.0×10^{39}	Nuclear region
		246	1009 ±112.3	4.5×10^{-12} 7.5×10^{39}	Whole galaxy
H2	13 34 30.46 -29 38 30.4	18	57.4 ±10	2.5×10^{-13} 4.2×10^{38}	Corresponding to IPC source I2
		18	37.4 ±10	1.7×10^{-13} 2.8×10^{38}	
H4	13 34 15.01 -29 36 1.9	18	30.4 ±9.6	1.3×10^{-13} 2.3×10^{38}	

^a Assuming $kT = 5 \text{ keV}$ and $N_{\text{H}} = 5 \times 10^{20} \text{ cm}^{-2}$.

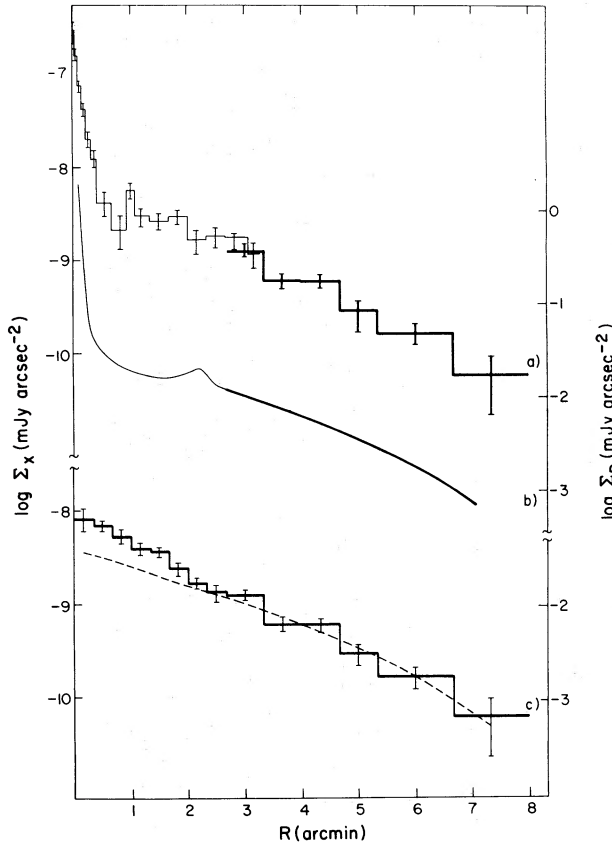


FIG. 5.—(a) Azimuthally averaged radial distribution of the background subtracted X-ray surface brightness (Σ_x). (light line): HRI data; (heavy line): IPC data (see text). (b) Azimuthally averaged radial distribution of the B band surface brightness, Σ_B . (light line): data from Talbot, Jensen, and Dufour (1979); (heavy line), optical data convolved through the IPC response. The units are shown on the right. (c) IPC (solid line) and convolved optical surface brightness profiles (dashed line). The normalization between the X-ray and optical profiles is arbitrary.

Figure 5b, is a combination of the raw optical data within $160''$ and their convolution with a Gaussian of $\sigma = 51''$ beyond $160''$, to match the resolution of the IPC portion of the composite X-ray surface brightness profile. The B band surface brightness profile is measured only to a radius of $\sim 360''$. The convolved profile was calculated out to $420''$ on the assumption that it follows the same exponential law outside $360''$ as in the measured part (Talbot, Jensen, and Dufour 1979). In Figure 5c the

convolved optical profile over the whole galaxy is compared to the IPC profile. From this figure a relative increase of Σ_x over Σ_B in the inner $120''$ region is apparent.

This effect can be seen in more detail from the ratio of the X-ray to the blue profiles shown in Figure 6. This shows the behavior of the monochromatic (2 keV) X-ray to optical (B band) flux ratio (f_x/f_B) as a function of radius from the galactic center. The ratio f_x/f_B is $(6.4 \pm 0.5) \times 10^{-8}$ in the nuclear region ($r = 10''$), has an average value of $(1.9 \pm 0.2) \times 10^{-7}$ in the region between $10''$ and $120''$, then decreases to $(1.0 \pm 0.1) \times 10^{-7}$ in the region between $120''$ and $360''$. The different f_x/f_B ratios in the inner $10''$ – $120''$ and the outer $120''$ – $360''$ regions cannot be due to a faulty normalization of the HRI and IPC profiles, since similar ratios are obtained when the IPC profile and the convolved blue light profiles are used (see Fig. 6).

A search for a correlation of the X-ray emission with the symmetric spiral arm structure gave negative results. As shown in Figure 7a, the HRI image was divided into 11 radial sectors of $16''$ incremental radius and 36 azimuthal sectors from $24''$ to $200''$ and into 12 azimuthal sectors in the outermost annulus of $44''$ width. For each annulus, an average surface brightness was calculated, and any of the azimuthal bins with a surface brightness above this average were plotted as shaded areas. As can be seen from Figure 7a, no concentration of these high surface brightness bins in the spiral arms is apparent. The average surface brightness in the spiral arm region is consistent with that of the interarm region, being $(7.3 \pm 1.1) \times 10^{-3}$ and $(6.7 \pm 0.7) \times 10^{-3}$ HRI counts arcsec^{-2} (after background subtraction), respectively. The 3σ upper limit on the excess HRI counts from the region of the arms is 239. This corresponds to an X-ray luminosity of $\sim 2 \times 10^{39}$ ergs s^{-1} for the spectral parameters of Table 3. The darkest bins in Figure 7a represent the bins in which the largest number of photons was detected. The concentration of these bins seems higher in a region near the inner part of the NE spiral arm and in a region $\sim 2'$ west of the nucleus. The former region is outside the H α spiral arms (see Fig. 9e of Jensen, Talbot, and Dufour 1981), but both are coincident with regions rich in young clusters (see Fig. 7b, also from Jensen, Talbot, and Dufour 1981).

III. DISCUSSION

The total X-ray luminosity of M83 ($L_x = 5.7 \times 10^{39}$ ergs s^{-1} , 0.5–3.0 keV) is typical of normal spiral galaxies (Fabbiano, Trinchieri, and Macdonald 1984). Both HRI and IPC observations show extended X-ray emission in the plane of the galaxy.

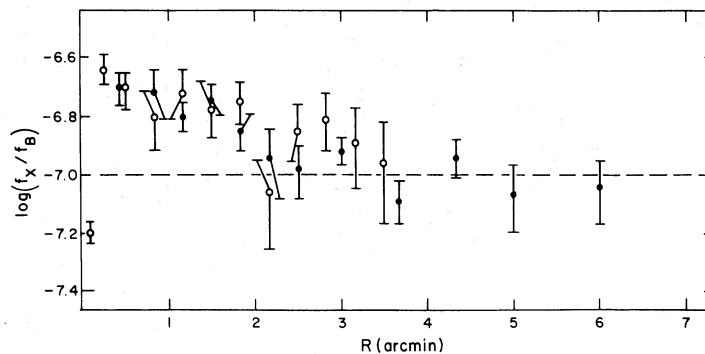


FIG. 6.—The ratio of X-ray to optical flux. (open circles): HRI and optical data; (filled circles): IPC and convolved optical data. The dashed line represents the average between $2'$ and $6'$.

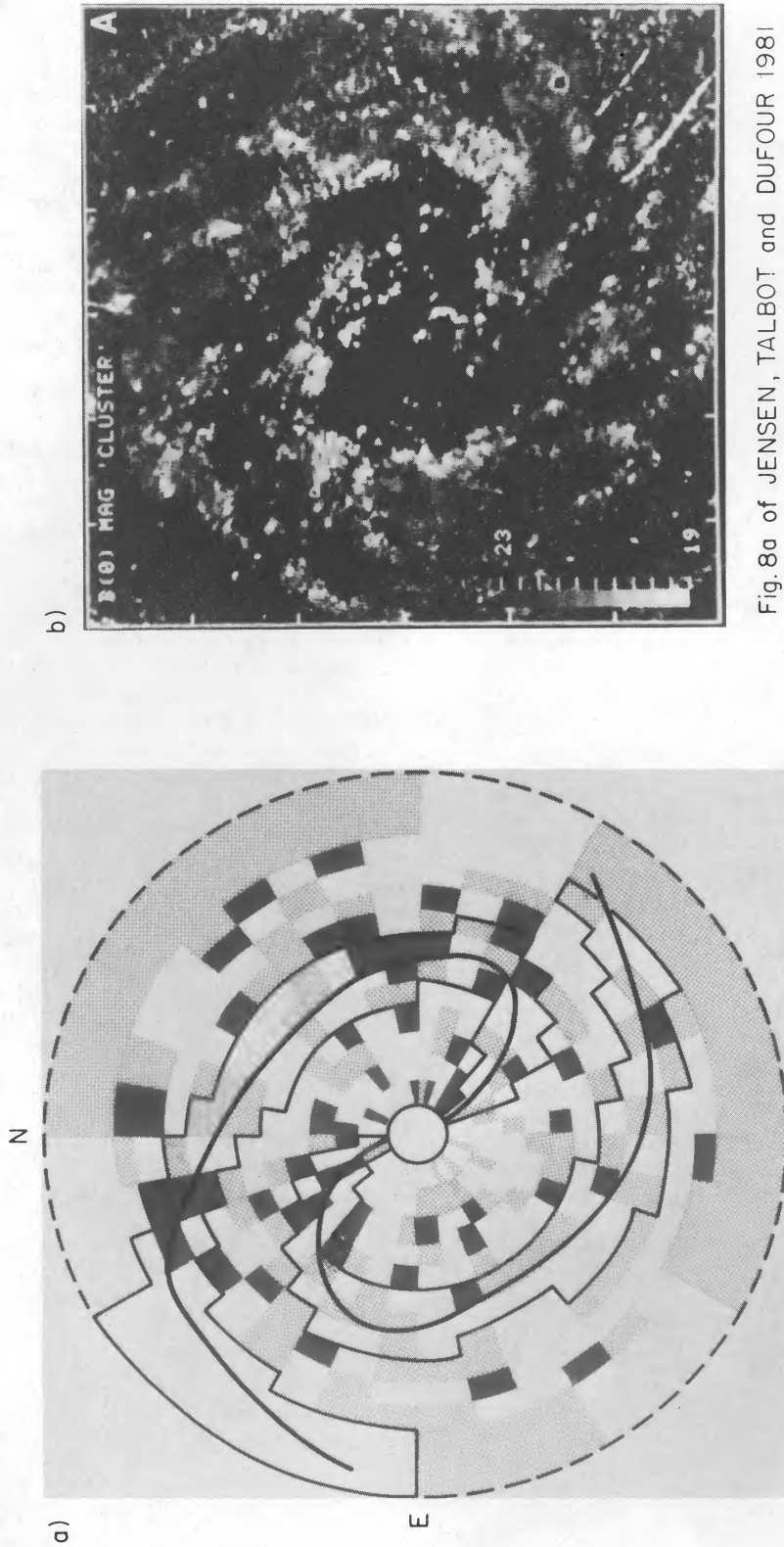


Fig. 8a of JENSEN, TALBOT and DUFOUR 1981

FIG. 7.—(a) Binning of the HRI image to search for spiral pattern. The image was divided in 11 radial sectors with 16" incremental radius and in 36 azimuthal sectors in the region between 24" and 200" from the nucleus. Only 12 azimuthal sectors were used in the outermost annulus. The shaded areas represent bins with surface brightness above to the average in the annulus. The darkest bins represent areas in which the largest number of photons were detected. A schematic representation of the spiral structure is also shown. (b) Map of the blue magnitude of the "young star clusters" from Fig. 8a of Jensen, Talbot, and Dufour (1981).

Three unresolved sources and a nuclear component are also detected in the HRI. The nuclear region alone accounts for $\sim 30\%$ of the total X-ray emission as seen in the HRI. The locations of the sources in M83 are shown in Figure 8.

a) Individual Sources and the Diffuse Emission

Three sources are detected with the HRI (in addition to the nuclear source), two of them very close to the nuclear region of M83 and one on a spiral arm. Three additional sources might also have been detected with the IPC. All these sources have fluxes greater than 1×10^{-13} ergs cm^{-2} s^{-1} . At the assumed distance of M83 (3.75 Mpc), their luminosity is in excess of 1×10^{38} ergs s^{-1} (see Table 3). The results of the *Einstein* medium survey (Gioia *et al.* 1984) indicate that the expected number of extragalactic serendipitous sources with $f_x >$

1×10^{-13} ergs cm^{-2} s^{-1} in the (0.3–3.5) band is ~ 0.3 in the area within the optical radius of M83 and is 0.1 for galactic sources. Therefore, the sources detected within the optical radius of M83 are most likely to be associated with this galaxy. A comparison with the map of the H II regions published by de Vaucouleurs, Pence, and Davoust (1983) and with the UV image (Bohlin *et al.* 1983) does not show any obvious counterpart for the X-ray sources. None of these sources is coincident with any of the four supernova remnants SN 1923a, SN 1950b, SN 1957d, or SN 1968e (de Vaucouleurs, de Vaucouleurs, and Corwin 1976) observed in M83. The upper limit on the X-ray luminosity of each of these supernova remnants is $\sim 1 \times 10^{38}$ ergs s^{-1} , higher than the typical X-ray luminosity of galactic remnants.

If the unresolved sources detected in M83 with $L_x >$

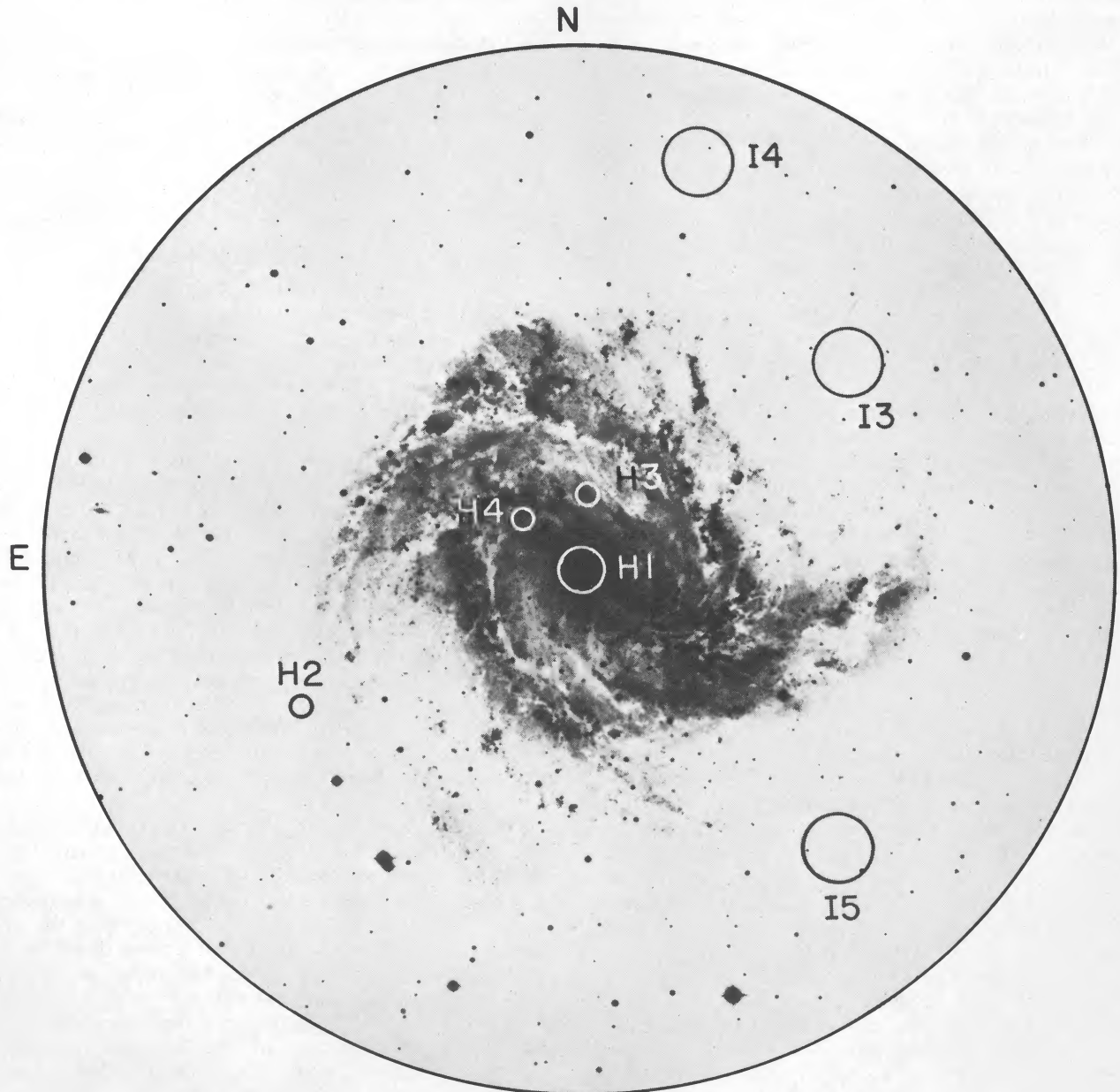


FIG. 8.—The position of the X-ray sources resolved in M83, superposed on a 40 minute exposure on IIIa J-B of the central region of M83 (courtesy of Dr. W. Wamsteker). The picture was obtained by Dr. S. Laustsen at the prime focus of the 3.6 m telescope at La Silla, ESO using a GG 385 filter. The IPC sources are indicated with a circle of $1'$ diameter; the HRI sources, with $14''$ diameter circles—a $40''$ diameter circle indicates the nuclear region. The outer circle has a diameter equal to the corrected isophotal diameter D_0 .

1×10^{38} ergs s^{-1} are indeed point sources, they represent the high end of the X-ray luminosity function of discrete sources in this galaxy. Their high X-ray luminosity suggests that they are close accreting binaries. The total X-ray luminosity of the bright sources detected in the HRI is about 20% of the luminosity of the diffuse component (excluding the nuclear region). Given the uncertainty in comparing the fluxes derived for the HRI and IPC sources, and given the better spatial resolution of the HRI, only the HRI results are used for this comparison. A similar ratio is found in M31 (Van Speybroeck *et al.* 1979) if the total luminosity of sources brighter than 1×10^{38} ergs s^{-1} is compared to that of fainter sources. This suggests that the diffuse X-ray emission from the plane of M83 is due to fainter unresolved sources. The total X-ray luminosity of the diffuse component in the HRI is $\sim 4.6 \times 10^{39}$ ergs s^{-1} (0.5–3.0 keV). This luminosity is sufficiently low to be easily explained with a collection of discrete X-ray sources like those observed in the Milky Way or in M31. As shown in Figure 5, the X-ray emission can be detected out to a radius of $\sim 8'$ from the nucleus, comparable with the revised photometric radius R_0 of Talbot, Jensen, and Dufour (1979).

Jensen, Talbot, and Dufour (1981) identify four components of the optical surface brightness distribution of M83: (a) the starburst nuclear region, occupying the inner $10''$ of the galaxy; (b) the spheroidal component, characterized by a surface brightness profile that follows the $R^{1/4}$ law and colors similar to those of elliptical galaxies, predominant in the region between $10''$ and $40''$; (c) the "old disk" or "smooth disk" (age $> 10^8$ yr) component, with exponential light distribution, responsible for most of the optical emission; and (d) the young stellar component (ages 10^6 – 10^8 yr), that closely follows the spiral pattern.

As discussed in § IIc, except for a possible association with star-forming regions in or near the inner spiral arms, the X-ray emission does not follow the spiral arm pattern. From the limit on the X-ray emission from the arm region, a contribution of less than 30% from sources associated with the young arm population cannot be excluded. However, most of the X-ray emission seems to originate rather uniformly in the plane of the galaxy. This suggests an association of the X-ray emission with the "smooth disk" and implies that a large fraction of the X-ray sources are probably associated with a population older than 10^8 yr. A small number of these sources could be capture binaries in the inner spheroidal component, as suggested for the "inner bulge" X-ray sources of M31 (Van Speybroeck *et al.* 1979) by van den Heuvel (1980). Globular cluster X-ray sources are also expected to contribute. Since M83 is seen face on, these sources would be seen projected on the plane, indistinguishable from the sources in it. Given the similarity of M83 to the Milky Way (see Jensen, Talbot, and Dufour 1981 and references therein) $\sim 10\%$ of the disk luminosity could be due to globular cluster sources. Most of the sources in the disk however are likely to be the product of the evolution of native binary systems belonging to the "smooth disk" population (see discussion in Fabbiano, Trinchieri, and Macdonald 1984).

As shown in Figure 6, the X-ray to optical flux ratios (f_x/f_B) are higher in the inner $2'$ region than in the outer $2'$ – $6'$ region. The different f_x/f_B ratios can be understood in part with a comparison of the X-ray emission of M83 to that of the Milky Way. As discussed in the literature (e.g., van den Heuvel 1980), the galactic X-ray sources can be divided into two classes, with different physical properties and different spatial distribution (see Giacconi 1974). The "type I" sources, or "disk sources,"

are typically associated with the galactic disk and spiral arms of the galaxy. They are commonly believed to be Population I massive binaries and have on average X-ray luminosities of the order of a few 10^{37} ergs s^{-1} . The "type II" sources, or "galactic bulge sources," have galactic longitude within 30° of the galactic center. The typical X-ray luminosities of the "type II" sources are $\sim 10^{38}$ ergs s^{-1} , assuming that they are located in the inner regions of the Milky Way (distances of 10–15 kpc). The same two classes of objects are observed also in M31 (Van Speybroeck *et al.* 1979). In M31, however, the "galactic bulge-type" X-ray sources are concentrated in a much smaller region of ~ 400 pc. The f_x/f_B ratio observed in the bulge region of M31 (~ 1 kpc radius) is 7×10^{-8} , higher than the X-ray to optical ratio for M31 as a whole (4.8×10^{-8}). Analogy with the Milky Way and M31 suggests that a concentration of "type II" or "galactic bulge-type" X-ray sources in the inner regions of M83 could explain the larger f_x/f_B ratio observed. A further contribution to the observed X-ray emission may also come from X-ray sources associated with the young stellar population. In Figure 7 there is an indication of a higher X-ray surface brightness in inner arm regions where a population of young stars is clustered. The age of these stars peaks at few 10^7 yr (Jensen, Talbot, and Dufour 1981). This is the time scale predicted from theoretical models for a massive binary system to evolve into an X-ray source (van den Heuvel 1980).

b) The Nuclear Region

Due to the complex optical morphology (W. Wamsteker 1984, private communication) of the nucleus of M83, its position cannot be determined accurately. However, the X-ray nuclear source lies within the boundaries of the extended radio, IR, optical, and UV sources detected in the nuclear region (Condon *et al.* 1982; Rieke 1976; Pastoriza 1975; Bohlin *et al.* 1983).

The observed X-ray luminosity of the nuclear region of M83 is 2×10^{39} ergs s^{-1} , for the spectral parameters of Table 3. The intrinsic X-ray luminosity, however, will be greater, if obscuring material is present in the nuclear region. Different methods for determining the visual extinction in M83 give different results. Bohlin *et al.* (1983) derive an $A_v = 1$ from the $H\alpha/H\beta$ ratio given by Pastoriza (1975). IR observations of the $10 \mu\text{m}$ silicate absorption feature (Lebofsky and Rieke 1979) imply a much larger value of the extinction ($A_v \approx 35$). The absorbing column that the X-ray source sees could then range from 3×10^{21} cm^{-2} to 9×10^{22} cm^{-2} (Jenkins and Savage 1984) implying that the X-ray luminosity of the nuclear region is likely to be greater than 2×10^{39} ergs s^{-1} . Further discussion of the extinction and an estimate of it from the X-ray data are given in § IIIc.

Observations in the far-infrared (Telesco and Harper 1980, and references therein) and in the ultraviolet (Bohlin *et al.* 1983; W. Wamsteker and G. G. C. Palumbo, in preparation) give evidence that the nuclear region of M83 is undergoing a burst of star formation. The $(U-B)_0$ color of the nuclear region of M83 is -0.51 , significantly bluer than that of the overall galaxy [$(U-B)_0 \approx -0.03$; Talbot, Jensen, and Dufour 1979], reinforcing the starburst picture.

The results of the X-ray observations also support a starburst model for the nucleus of M83. The X-ray luminosity of the nuclear region is consistent with that of other known starburst nuclei, such as NGC 7714 ($L_x = 6 \times 10^{40}$ ergs s^{-1} ; Weedman *et al.* 1981), NGC 253 ($L_x = 3 \times 10^{39}$ ergs s^{-1} ; Fabbiano and Trinchieri 1984), and M82 ($L_x = 7.4 \times 10^{39}$ ergs

s^{-1} ; Watson, Stanger, and Griffiths 1983). Moreover, the ratio of X-ray to H α emission for M83 is $\log(L_x/L_{H\alpha}) = -1.26$. This is similar to what is seen in NGC 7714 for which one obtains $\log(L_x/L_{H\alpha}) = -1.22$, using the values in Weedman *et al.* (1981). This ratio is different from the typical values seen in active Seyfert-like nuclei, the average value for active galaxies being $+1.15$ (Steiner 1981). Elvis and Van Speybroeck (1982) found $\log(L_x/L_{H\alpha}) = +1.92$ for the low-luminosity active nucleus of M81.

Since the nucleus of M83 is a starburst, one could expect its X-ray to optical flux ratio to be enhanced with respect to that of normal galaxies as in the case of blue star-forming galaxies (Fabbiano, Feigelson, and Zamorani 1982). These authors showed that the range of values of f_x/f_B observed in these latter galaxies is 10^{-7} to 10^{-5} and $f_x/f_B \approx 10^{-6}$ for galaxies with $(U-B)_0 \approx -0.5$. However, $f_x/f_B = 6.4 \times 10^{-8}$ in the inner $10''$ of M83. The intrinsic f_x/f_B is likely to be even lower due to the effect of the extinction (see discussion in § IIIc). This would make the difference between f_x/f_B in the nucleus of M83 and the values for both the blue galaxies and the main body of M83 even more pronounced. This low f_x/f_B therefore indicates a different X-ray emitting population in the starburst nucleus of M83. This suggests that only a very small fraction of the X-ray emission of the nuclear region of M83 is likely to be produced by evolved objects like binary X-ray sources.

The stellar population derived assuming reasonable starburst models cannot produce all of the observed X-ray luminosity of the nucleus. Bohlin *et al.* (1983) applied to the nucleus of M83 the models that Rieke *et al.* (1980) applied to the nucleus of M82, scaling them to match the far-IR luminosity observed in M83. They found that only models A, G, and H of Rieke *et al.* give acceptable results for M83. These models give $\sim 2 \times 10^5$ stars with masses $M > 10 M_\odot$ for the nucleus of M83. Model A also gives $\sim 7 \times 10^6$ stars with masses in the range $0.8\text{--}2 M_\odot$. The stellar contribution to the nuclear X-ray emission would then be about 3×10^{38} ergs s^{-1} at most, if an $L_x \sim 10^{33}$ ergs s^{-1} is assumed for the most massive stars (see Vaiana *et al.* 1981) and an $L_x \approx 10^{31}$ ergs s^{-1} is assumed for the young G type stars (see Micela *et al.* 1984). At the estimated supernova rate of $\sim 1\text{--}4$ SN per century, young supernova remnants could contribute a similar amount; the total X-ray luminosity for the nuclear region would then be less than 10^{39} ergs s^{-1} , more than a factor of 2 lower than the observed luminosity, uncorrected for internal extinction.

However, if the occurrence of outflowing gas that is seen in the X-ray emission of M82 (the "halo"; Watson, Stanger, and Griffiths 1984) and NGC 253 (the "jetlike" feature; Fabbiano and Trinchieri 1984) is a common feature of starburst nuclei, then a fraction of the HRI counts detected in the nuclear region of M83 could come from such a feature. Strong evidence of gas outflow from the nuclear region of M83 is given by the presence of absorption lines blueshifted by 1000 km s^{-1} relative to the system's velocity (Bohlin *et al.* 1983). Since M83 is seen face on, the outflowing gas would be seen projected on the nucleus. The ratio of the counts detected in the nuclear source to those in the diffuse component around it is ~ 0.2 for NGC 253. If the same scaling factor is used for the nuclear region of M83, the intrinsic luminosity could be a factor of ~ 5 lower than estimated earlier in this section. Since NGC 253 has similar physical parameters and nearly the same morphology as M83 (de Vaucouleurs, Pence, and Davoust 1983), this is probably a reasonable assumption. The resulting nuclear luminosity would be $\sim 4 \times 10^{38}$ ergs s^{-1} , for the spectral parameters of

Table 2, consistent with the estimated luminosity of the stellar population. If the X-ray spectrum is softer than a thermal bremsstrahlung spectrum with $kT = 5$ keV, as would be expected if binary X-ray sources are not present, then the nuclear X-ray luminosity could be somewhat lower.

The relative absence of an evolved X-ray emitting population in the nuclear region can be used to set constraints on the age of the burst of star formation. The time for a close binary system with a primary of mass larger than about $15 M_\odot$ to reach the X-ray emitting stage is estimated at $\sim 10^7$ yr (see review by van den Heuvel 1980). Therefore the burst of star formation probably happened as recently as $\sim 10^7$ yr ago, so that only a small fraction of the very massive stars had time to evolve into X-ray sources. This is consistent with the burst ages of the Rieke *et al.* (1980) models. Similar conclusions were reached for the galaxy NGC 5253 by Moorwood and Glass (1982) and for NGC 5204 by Fabbiano and Panagia (1983).

An estimate of the X-ray luminosity of the hot gas outflowing from the nucleus of M83 can be obtained assuming that $\sim 4/5$ of the counts detected in the nuclear region are due to this component, as observed in NGC 253 (Fabbiano and Trinchieri 1984). Bohlin *et al.* (1983) estimate a velocity of $\sim 1000 \text{ km s}^{-1}$ for the gas. The deprojected velocity is $v \approx 1100 \text{ km s}^{-1}$, for an inclination angle $i = 24^\circ$. For a corresponding $T \approx 9 \times 10^7$ K and hydrogen column density of $5 \times 10^{20} \text{ cm}^{-2}$, this gas would have $L_x \approx 1.6 \times 10^{39}$ ergs s^{-1} . This luminosity is consistent with what is expected if all the gas ejected from the nucleus is radiating by thermal emission at a temperature of 9×10^7 K. Bohlin *et al.* (1983) estimate an ejection rate of $\gtrsim 0.1 M_\odot \text{ yr}^{-1}$. If the age of the burst is $\sim 10^7$ yr, $10^6 M_\odot$ of gas have been ejected from the nucleus. If the gas is ejected symmetrically in the direction perpendicular to the plane, only one-half of it would be along the line of sight, projected on the nucleus. With the above conditions, the X-ray luminosity of the gas would be $L_x \approx 1.4 \times 10^{39}$ ergs s^{-1} , on the assumption that the gas uniformly fills a volume of $\sim 4 \times 10^{63} \text{ cm}^3$ (the volume occupied by the gas ejected from the nucleus of NGC 253; Fabbiano and Trinchieri 1984). The cooling time of the ejected gas would be $\sim 4.3 \times 10^8$ yr (see Tucker 1975).

c) The Extinction in the Nuclear Region

As remarked in § IIIb, different methods for deducing the extinction in the nuclear region give different values, $A_v = 1$ from the H α /H β ratio (Bohlin *et al.* 1983), and $A_v = 35$ from the $10 \mu\text{m}$ silicate absorption feature (Lebofsky and Rieke 1979). This discrepancy could be understood in part if the dust present in the nuclear region were distributed nonhomogeneously throughout the source. In this case the average column seen by the extended optical source would be less than that in the clouds detected in the infrared. Moreover, the observed H α /H β ratio could be contaminated by backscattering into the beam (Jones and Stein 1975). This would reduce the amount of optical extinction derived.

The effect of the extinction on the f_x/f_B ratio is a function of the X-ray spectrum. For a "hard" X-ray spectrum ($kT \gtrsim 1$ keV), the presence of an absorbing column would affect much more severely the optical than the X-ray flux. As a consequence, the intrinsic f_x/f_B ratio would be smaller than the one observed. Conversely, for a very "soft" X-ray spectrum ($kT \ll 1$ keV), the X-ray flux would be affected more severely than the optical flux, resulting in an intrinsic f_x/f_B larger than the one observed. A graphical representation of this is given in

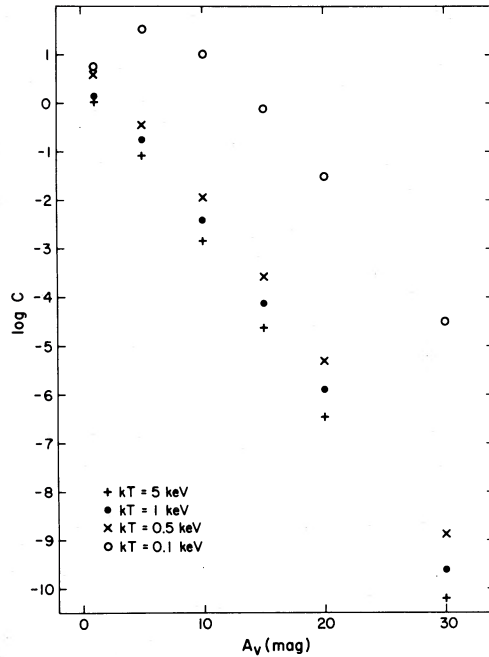


FIG. 9.—The correction factor “c” for the f_x/f_B ratio as a function of extinction A_v , calculated assuming a thermal bremsstrahlung spectrum for the X-ray emission.

Figure 9, where the ratio of the intrinsic to the observed f_x/f_B (correction factor “c”) is shown as a function of extinction A_v for four temperatures.

An estimate of the amount of absorbing material in the nuclear region can be obtained by comparing the X-ray to optical flux ratio of the nuclear region of M83 with the observed f_x/f_B for stars. In our monochromatic flux units, the f_x/f_B ratios for early stars range from $\sim 10^{-6}$ to $\sim 10^{-11}$ (Vaiana *et al.* 1981). Early-type stars have a typical X-ray temperature $kT \approx 1$ keV (R. Harnden 1984, private communication). If no correction for intrinsic extinction is applied, $f_x/f_B \approx 4 \times 10^{-8}$ for the nucleus of M83 for an X-ray spectrum with $kT = 1$ keV. For the intrinsic nuclear f_x/f_B to equal the lower value of f_x/f_B observed for stars ($f_x/f_B \approx 10^{-11}$), “c” needs to be $\sim 2.5 \times 10^{-4}$. This corresponds to ~ 13 magnitudes of extinction (see Fig. 9).

This represents a conservative estimate on the nuclear extinction for the following reasons. This limit was achieved by equating the intrinsic nuclear f_x/f_B to the lowest boundary of the f_x/f_B distribution for stars. On average, however, stars have much higher X-ray to optical ratios (see Vaiana *et al.* 1981). Moreover, as discussed above, the stellar contribution could only account for a fraction of the nuclear X-ray flux. If few evolved X-ray sources are present, they would have an X-ray spectrum harder than the stellar one and a higher intrinsic f_x/f_B ($\sim 10^3$ higher than stars). Thus the limit on A_v would have to be smaller, to be consistent with the constraints imposed by the f_x/f_B ratio. Finally, if hot gas emission contributes significantly to the X-ray flux of the nuclear region, as discussed in § IIIb, the nuclear f_x/f_B could be about one-fifth of the value used in this calculation, thus implying an even smaller A_v .

The derived limit on the extinction is already much lower than the value $A_v = 35$ derived from IR measurements by Lebofsky and Rieke (1979). This could be a further indication of a nonhomogeneous distribution of the dust in the region.

IV. CONCLUSIONS

Detailed X-ray observations of M83 provide for the first time the opportunity to study the distribution of X-ray sources in a face-on spiral galaxy similar to the Milky Way. The main results can be summarized as follows:

1. Three bright sources ($L_x > 1 \times 10^{38}$ ergs s^{-1}) are resolved in the HRI observation. Diffuse X-ray emission is also detected in the plane of the galaxy. This emission is probably due to individual sources, each fainter than about 10^{38} ergs s^{-1} , distributed uniformly in the disk and arms of the galaxy.

2. Comparison of the X-ray and optical radial profiles shows a relative excess of X-ray emission in the inner 2' region, most likely due to a concentration of bulge-type X-ray sources. A similar situation is observed in M31 and in the Milky Way, where the bulge sources have on average a higher X-ray luminosity than the disk sources.

3. The starburst nucleus of M83 is a strong X-ray source with $L_x \approx 2 \times 10^{39}$ ergs s^{-1} . However, its X-ray to optical flux ratio f_x/f_B is significantly lower than the f_x/f_B ratios observed in blue star-forming galaxies (Fabbiano, Feigelson, and Zamorani 1982) and in the main body of the galaxy. This suggests that the X-ray emission from the nucleus of M83 is not dominated by the contribution of massive binary systems, but is due to a less evolved X-ray emitting population. The age of the burst is thus $\sim 10^7$ yr.

4. The young star and supernova remnant population predicted by the models of Rieke *et al.* (1980) would give an X-ray luminosity of $\sim 6 \times 10^{38}$ ergs s^{-1} , therefore only partially explaining the emission from the nuclear region. However, the 1000 km s^{-1} blueshifted absorption lines in the UV spectrum of the nucleus (Bohlin *et al.* 1983) strongly suggest gas outflow. Thermal emission from hot shock-heated gas ejected from the nucleus along the line of sight could account for a large fraction of the nuclear X-ray luminosity. Such hot outflowing gas has been detected in the X-ray emission of M82 (Watson, Stanger, and Griffiths 1984) and NGC 253 (Fabbiano and Trinchieri 1984).

5. The X-ray data put a limit on the amount of extinction in the nuclear region of M83. The derived upper limit $A_v < 13$ is significantly lower than the $A_v = 35$ derived from the $10 \mu m$ silicate absorption feature (Lebofsky and Rieke 1979). The discrepancy can be understood if the dust in the region is distributed nonhomogeneously.

We wish to thank Dr. G. de Vaucouleurs and Dr. W. Wamsteker for kindly providing us with copies of the optical image of M83 and Susan Gibbs for help in the data analysis. G. G. C. P. acknowledges the use of data from the *Einstein* Data Bank and thanks the Italian Piano Spaziale Nazionale for partial financial support. This work was supported under NAS contract NAS8-30751.

REFERENCES

- Bohlin, R. C., Cornett, R. H., Hill, J. K., Smith, A. M., and Stecker, T. P. 1983, *Ap. J. (Letters)*, **274**, L53.
- Condon, J. J., Condon, M. A., Gisler, G., and Puschell, J. J. 1982, *Ap. J.*, **252**, 102.
- de Vaucouleurs, G. 1979, *A.J.*, **84**, 1270.
- de Vaucouleurs, G., de Vaucouleurs, A., and Corwin, H. G. 1976, *Second Reference Catalogue of Bright Galaxies* (Austin: University of Texas Press).
- de Vaucouleurs, G., Pence, W. D., and Davoust, E. 1983, *Ap. J. Suppl.*, **53**, 17.
- Dufour, R. J., Talbot, R. J., Jensen, E. B., and Shields, G. A. 1980, *Ap. J.*, **236**, 119.
- Elvis, M., and Van Speybroeck, L. 1982, *Ap. J. (Letters)*, **257**, L51.
- Fabbiano, G., Feigelson, E., and Zamorani, G. 1982, *Ap. J.*, **256**, 397.
- Fabbiano, G., and Panagia, N. 1983, *Ap. J.*, **266**, 568.
- Fabbiano, G., and Trinchieri, G. 1984, *Ap. J.*, **286**, 491.
- Fabbiano, G., Trinchieri, G., and Macdonald, A. 1984, *Ap. J.*, **284**, 65.
- Giacconi, R. 1974, in "X-ray Astronomy," ed. R. Giacconi and H. Gursky (Dordrecht: Reidel), p. 155.
- Giacconi, R., et al. 1979, *Ap. J.*, **230**, 540.
- Gioia, I., et al. 1984, *Ap. J.*, **283**, 495.
- Harnden, F. R., Fabricant, D. G., Harris, D. E., and Schwarz, J. 1984, "Scientific Specifications of the Data Analysis System for the *Einstein* Observatory (*HEAO 2*) IPC", Internal SAO Special Report 393.
- Heiles, C. 1975, *Astr. Ap. Suppl.*, **20**, 37.
- Jenkins, E. B., and Savage, B. D. 1974, *Ap. J.*, **187**, 243.
- Jensen, E. B., Talbot, R. J., and Dufour, R. J. 1981, *Ap. J.*, **243**, 716.
- Jones, C., and Forman, W. 1984, *Ap. J.*, **276**, 38.
- Jones, T. W., and Stein, W. A. 1975, *Ap. J.*, **197**, 297.
- Lebofsky, M. J., and Rieke, C. H. 1979, *Ap. J.*, **229**, 111.
- Micela, G., et al. 1984, preprint.
- Moorwood, A. F. M., and Glass, I. S. 1982, *Astr. Ap.*, **115**, 84.
- Pastoriza, M. G. 1975, *Ap. Space Sci.*, **33**, 173.
- Rieke, G. H. 1976, *Ap. J. (Letters)*, **206**, L15.
- Rieke, G. H., Lebofsky, M. J., Thompson, R. I., Low, F. J., and Tokunaga, A. T. 1980, *Ap. J.*, **238**, 24.
- Sersic, J. L., and Pastoriza, M. 1967, *Pub. A.S.P.*, **79**, 152.
- Steiner, J. 1981, *Ap. J.*, **250**, 469.
- Talbot, R. J., Jensen, E. B., and Dufour, R. J. 1979, *Ap. J.*, **229**, 91.
- Telesco, C. M., and Harper, D. A. 1980, *Ap. J.*, **235**, 392.
- Topka, K., et al. 1982, *Ap. J.*, **259**, 677.
- Tucker, W. H. 1975, *Radiation Processes in Astrophysics* (Cambridge, Mass.: MIT Press), pp. 206, 207.
- Vaiana, G., et al. 1981, *Ap. J.*, **245**, 163.
- van den Heuvel, E. P. J. 1980, in *X-Ray Astronomy*, ed. R. Giacconi and G. Setti (Dordrecht: Reidel), p. 119.
- Van Speybroeck, L., Epstein, A., Forman, W., Giacconi, R., Jones, C., Liller, W., and Smarr, L. 1979, *Ap. J. (Letters)*, **234**, L45.
- Watson, M., Stanger, V., and Griffiths, R. E. 1984, *Ap. J.*, **286**, 144.
- Weedman, D. W., Feldman, F. R., Balzano, W. A., Ramsey, L. W., Sramek, R. A., and Wu, C.-C. 1981, *Ap. J.*, **248**, 105.

G. FABBIANO and G. TRINCHIERI: Harvard-Smithsonian Center for Astrophysics, 60 Garden Street, Cambridge, MA 02138

G. G. C. PALUMBO: Istituto T.E.S.R.E./CNR, via De' Castagnoli 1, 40126 Bologna, Italy